Communication

Diffusion Bonding of Al7075 to Ti-6Al-4V by Spark Plasma Sintering and Using a Copper Interlayer

Abdulaziz Alhazaa [1,2,*], **Hamad Albrithen [1,2]**, **Mahmoud Hezam [2,3]**, **Muhammad Ali Shar [2]**, **Ibrahim Alhwaimel [1]**, **Yasser Alharbi [2]** and **Claude Estournes [4,*]**

[1] Department of Physics and Astronomy, College of Science, King Saud University, Riyadh 11451, Saudi Arabia
[2] King Abdullah Institute for Nanotechnology, King Saud University, Riyadh 11451, Saudi Arabia
[3] Physics Department, College of Science, Imam Mohammad Ibn Saud Islamic University (IMSIU),
   Riyadh 13318, Saudi Arabia
[4] CIRIMAT, CNRS-INP-UPS, Université Toulouse 3-Paul Sabatier, 118 route de Narbonne,
   31062 Toulouse, France
* Correspondence: aalhazaa@ksu.edu.sa (A.A.); estournes@chimie.ups-tlse.fr (C.E.)

Abstract: Sheets of aluminum 7075 and titanium Ti-6Al-4V alloys were successfully joined using the spark plasma sintering (SPS) process. A copper foil was placed as an interlayer between the two surfaces. The bonding was made at 480 °C, 500 °C, and 520 °C with a holding time of 10 min and under a uniaxial pressure of 5 MPa and 10 MPa. The obtained bonds were analyzed by scanning electron microscopy, energy dispersive spectroscopy (SEM/EDS), and wavelength dispersive spectroscopy (WDS). It was found that copper diffused away through Al7075 and formed Al_2Cu intermetallics but was not present at the joint region. The investigation of the fractured surfaces using X-ray diffraction (XRD) showed that the joint region contained $TiAl_3$, $TiAl_2$, and Ti_3Al intermetallic compounds. The presence of the Cu foil was believed to hinder the formation of Al_3Ti observed in previous studies by allowing more Ti to diffuse into the Al side.

Keywords: spark plasma sintering; diffusion; intermetallic compounds

1. Introduction

Solid-state diffusion bonding of aluminum and its alloys to other dissimilar metals like titanium poses a challenge due to the fact that aluminum surfaces tend to build a thick protective oxide layer that prevents metal-to-metal contact and therefore makes the joining process difficult to achieve [1–3]. The oxide layer for aluminum gets thicker and more stable at elevated temperature and even under vacuum [1]. However, the use of certain interlayers has shown to be successful in disturbing the oxide film and helping to facilitate the direct metal-to-metal contact, thereby producing solid joints between aluminum and dissimilar metals, such as titanium alloys. For example, Al7075 alloy was joined with Ti-6Al-4V alloy using a diffusion bonding process after coating both surfaces with Cu under an acidic solution in an electrodeposition process. The acidic environment during the Cu coating process was essential to remove the oxide layer prior to Cu electrodeposition [3]. Therefore, it will be an aim to join Al7075 to Ti-6Al-4V in a simpler process without this prior electrodeposition process.

The spark plasma sintering (SPS) technique is an efficient low-temperature bonding method that uses high-energy DC pulses to provide the heating source for the consolidation process [4,5]. In addition to providing a rapid joule heating, these high-energy DC pulses can generate local sparks or even plasma discharges at the grain boundaries of the powder particles, resulting in both surface cleaning of adsorbed species and oxide layer removal [4,6–8].

Although spark plasma sintering technology (SPS) was primarily invented to sinter powder to bulk materials, it was proven to have other functions, including sheet joining

and functioned graded materials (FGM) joining [9–11]. For example, SPS was successfully used in many research projects to bond dissimilar bulk alloys which have complex shapes, relying on the fact that the DC pulses efficiently pass across the intimate surfaces and therefore activate atomic diffusion, resulting in better uniformity at the joint interfaces. Furthermore, sparks created between the mating surfaces helped to remove the remaining oxide films during the SPS process [11,12].

In this study, we applied SPS to bond Al7075 to Ti-6Al-4V alloy using a Cu interlayer; we noted the effect of using copper to facilitate the joining of aluminum to titanium and studied a possible intermetallic formation at the joint region.

2. Materials and Methods

Al7075 and Ti-6Al-4V alloys were purchased from Goodfellow in the form of extruded cylindrical rods. The diameter of the rods was 10 mm, which was similar to the inner diameter of the graphite die. Each rod was sliced by a diamond cutter to produce many identical samples of a thickness of 0.5 cm. Every sample was ground starting from 80 grit to 1000 grit using SiC sandpaper. Then, they were polished down using aluminum oxide suspension to 1 micrometer. The surfaces were then ultrasonically cleaned in acetone for 10 min, then in ethanol for 20 min, and then kept in desiccators prior to the SPS process. A 100 μm copper foil with purity of 99.99% was used as the interlayer.

The samples were loaded into the graphite die that was inserted inside the chamber of a field-assisted sintering technology (FAST) unit (SPS-210 Sx from SUGA Co., Ltd., Tokyo, Japan) for sintering at a holding temperature of 480 °C, 500 °C, and 520 °C, respectively, for three different samples under 5–10 MPa pressure with a vacuumed atmosphere of 7 Pa and a holding time of 10 min. The reason behind the choice of this range of temperature was because the Al7075/Cu eutectic phase was observed in a previous study [2]. The heating rate was 100 °C per minute.

For each bonding experiment, once the bonding time was reached the bonded sample was left to cool down under vacuum to ambient temperature and then taken out from the chamber. The bonded samples were cut across to the joint plane and then mounted in Bakelite powder (Buehler, Lake Bluff, IL, USA) for easier handling during metallurgical preparations. The bonded samples were ground with SiC paper down to grade 1200 and polished in Al_2O_3 suspension down to 1 μm. A JSM-7600F scanning electron microscope (SEM) (Joel, Tokyo, Japan) was used to characterize the microstructure. An X-ray diffraction (X'Pert Pro X-ray diffractometer, PAnalytical, Almelo, The Netherlands) was used to study the present crystallographic phases due to sintering. Electron probe X-ray microanalysis (EPMA) using wavelength dispersive spectrometry (WDS) was performed on different spots located across the interfaces in order to investigate the elemental compositions. At each spot location, background correction was first performed relative to the corresponding intensities of the reference materials before composition calculations were performed. The matrix correction software CITZAF was used to process the measured intensity ratios and yield the actual compositions [13]. The strength of the bonds was evaluated using a compressive machine (Instron 5969) from Norwood, MA, USA with a load cell of 5 kN and ramp rate of 1 mm/min. One sample was used for each process condition. The stress corresponding to the maximum load (load at fracture) was evaluated using Bluehill 3.22.1373 software from Norwood, MA, USA.

3. Results and Discussion

3.1. SEM and EPMA Analysis

Whenever the sintering conditions were good, adherence was observed between the two alloys, with no porosity observed at the interface. An interphase layer of a few microns in thickness, more or less continuous, was observed, the nature of which will be identified later in the paper.

Figure 1 shows the bonded samples using a Cu interlayer at the different temperatures of 480 °C, 500 °C, and 520 °C for 10 min. It is evident, as expected, that with increasing

bonding temperature the diffused copper through the aluminum side reached farther from the aluminum–titanium interface. At 480 °C, Cu diffused by not more than 5 μm along the interface. When the temperature was increased to 500 °C, Cu diffused remarkably farther in some regions, reaching ~5–75 μm inside the Al7075 region. At 520 °C, all the copper had diffused to large distances (>70 μm) far from the interface.
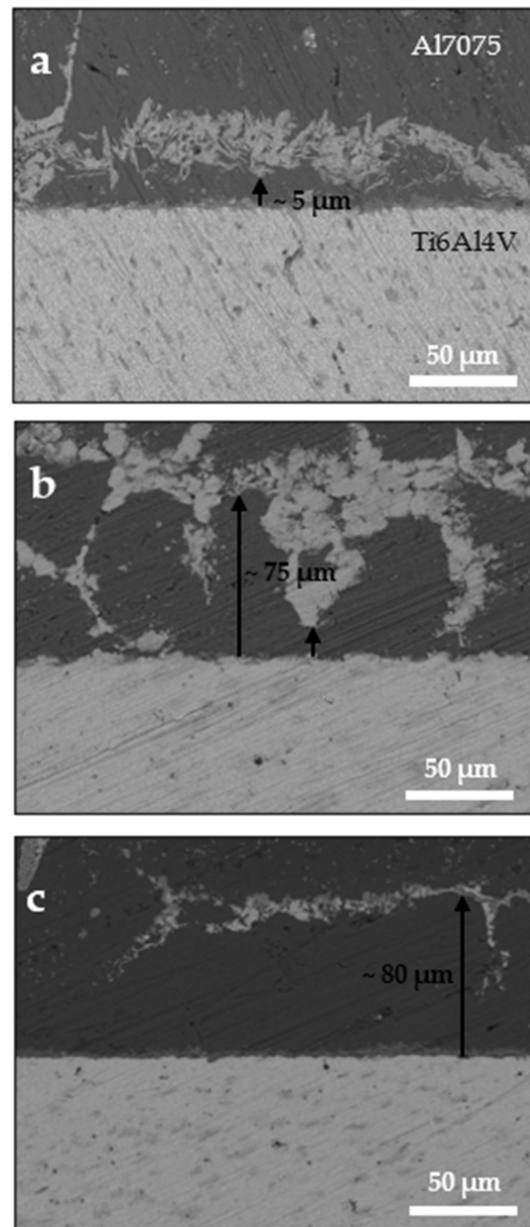

Figure 1. FE-SEM images of the Al7075/Ti-6Al-4V interface with Cu interlayer at 10 MPa and (**a**) 480 °C, (**b**) 500 °C, and (**c**) 520 °C, with a holding time of 10 min.

The holding pressure also played a significant role in the diffusion of copper. Figure 2 shows the SEM images at two different holding pressures: 5 MPa and 10 MPa both at 520 °C and 10 min holding time. Clearly, the copper diffusion through the aluminum was enhanced with the increase in holding pressure. While at 10 MPa all the Cu was diffused to >70 μm from the interface, the Cu was less diffused under 5 MPa, and it was in fact still adjacent to the interface in many regions.
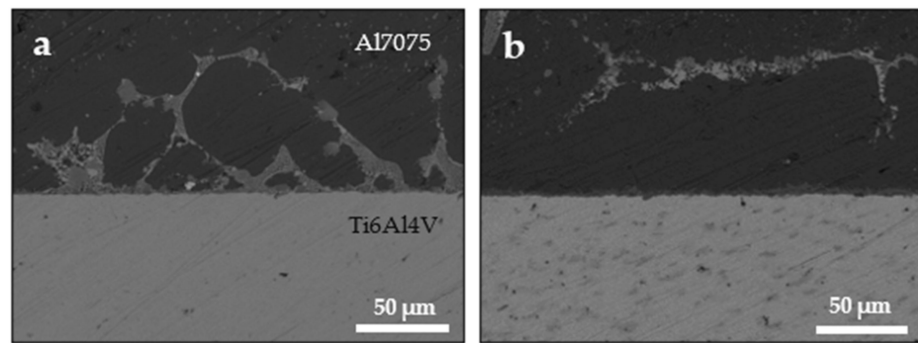
Figure 2. FE-SEM images of the Al7075/Ti-6Al-4V interface with Cu interlayer at 520 °C and holding pressure of (**a**) 5 MPa and (**b**) 10 MPa, with a holding time of 10 min for both samples.

A selected SEM image that belonged to the bond made at 520 °C was used for WDS quantitative analysis measuring the atomic percentages of Al, Ti, and Cu for various regions. Figure 3a shows the joint region at which higher magnification images were taken and used for EPMA-WDS analysis (shown as red rectangles). Figure 3b,c show higher magnification images of, respectively, the joint region and the region with diffused Cu in the aluminum side. The labelled regions were analyzed by EPMA-WDS. Region 1 indicated 73.5 at% of Al and 26.5 at% of Ti, suggesting that this region contained an intermetallic formation based only on aluminum and titanium at the aluminum side of the joint region. The analysis of region 2 showed less aluminum (59 at%) and higher titanium (41 at%) compared to region 1, suggesting a possible formation of a mixture of $TiAl_3$, $TiAl_2$, Ti_3Al, or TiAl along the titanium side. The exact intermetallic compounds formed were identified by X-ray diffraction in the following section. No significant copper phases were observed at the joint region. In Figure 3c, two interesting regions were observed. Region 3 gives a typical atomic percentage of the $\theta(Al_2Cu)$ phase with 67 at% of aluminum and 32.5 at% of Cu. On the other hand, the analysis of region 4 gives the eutectic composition of Cu and Al as approximately a 50 to 50 atomic percentage.
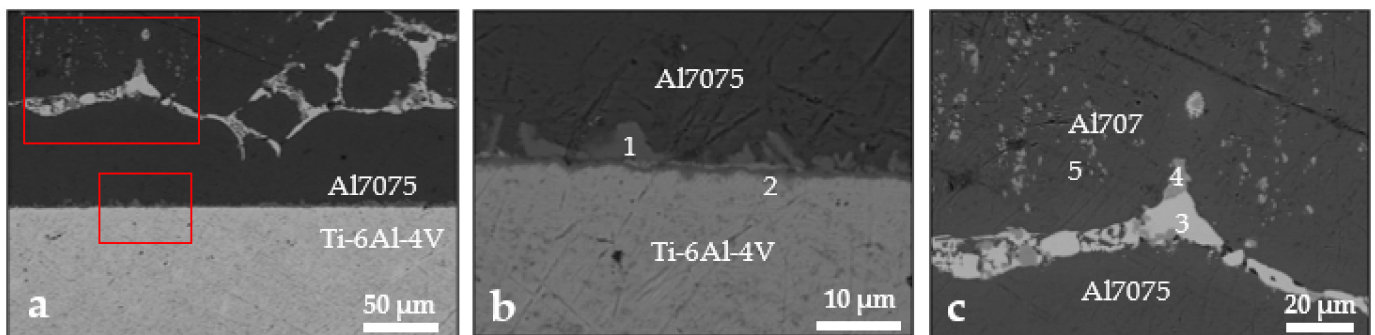

Figure 3. Microstructure of the Al7075/Ti-6Al-4V interface with Cu interlayer at 520 °C, holding pressure of 10 MPa, and holding time of 10 min at (**a**) low magnification at the joint region, at higher magnification (**b**) at the joint region, and at (**c**) diffused copper in the Al side. The magnified areas in (**b**,**c**) are shown as red rectangles in (**a**).

3.2. X-ray Diffraction and EDS of the Fractured Surfaces

XRD analysis was performed on the fractured surfaces of both Ti and Al sides. Figures 4 and 5 show the XRD patterns of the aluminum and titanium surfaces after fracturing the bond for the sample bonded at 520 °C. The intermetallic compounds (IMCs) formed on the aluminum side were identified to be $TiAl_3$ (JCPDS file No. 37-1449), Ti_3Al (JCPDS file No. 52-0859), and $TiAl_2$ (JCPDS file No. 52-0861). The pure Al peaks were indexed according to the JCPDS file No. 04-0787. The same IMCs were also detected at the Ti side, where the pure Ti peaks were indexed according to the JCPDS file No. 44-1294. A remarkable observation was the absence of any Cu-based structure even at the aluminum

side. This indeed confirms the above SEM and WDS observations that copper deeply diffused into the aluminum side, obstructing the contribution to the XRD signal. Although copper was inserted as a foil in between the two mating surfaces, the copper seemingly diffused away through the aluminum and formed a eutectic reaction and intermetallic phase but had no contribution to the mechanism of joining.
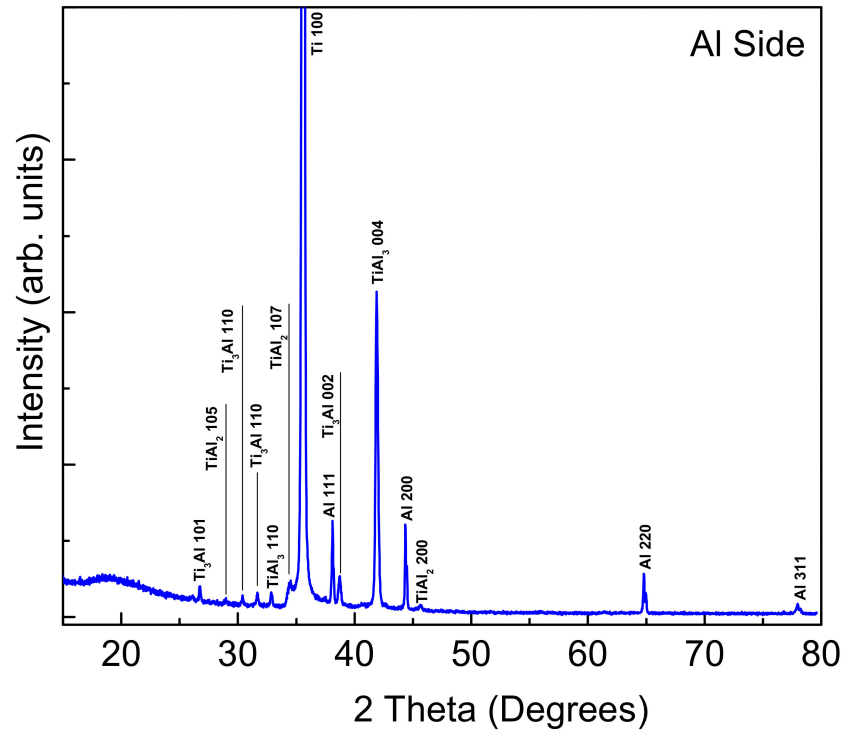

Figure 4. XRD pattern of the fractured surface (Al7075 side) for the sample bonded at 520 °C, holding pressure of 10 MPa, and holding time of 10 min.
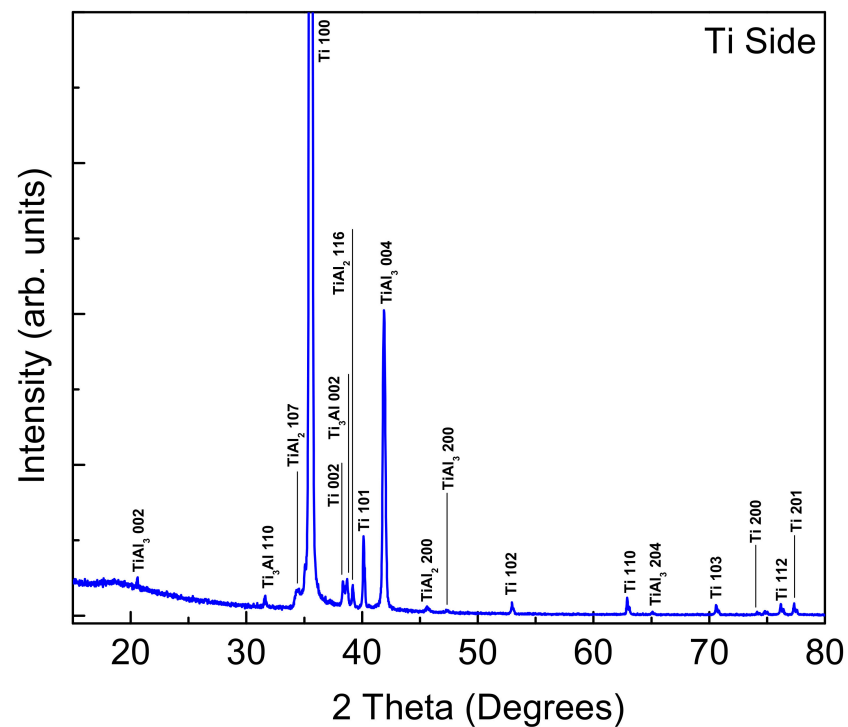

Figure 5. XRD pattern of the fractured surface (Ti-6Al-4V side) for the sample bonded at 520 °C, holding pressure of 10 MPa, and holding time of 10 min.

EDS analysis of the fractured surfaces of the bond made at 520 °C with a holding pressure of 10 MPa was performed and is shown in Figure 6. SEM images shows a brittle-like fracture that indicates the fracture occurred within the intermetallic compounds. The EDS area scan of the aluminum fractured surface showed 75 wt% of Al and 24 wt% of Ti. The EDS area scan of the Ti fractured surface showed 59 wt% of Al and 40 wt% of Ti. This EDS result was expected as the joint region was dominated by Al-Ti IMCs.
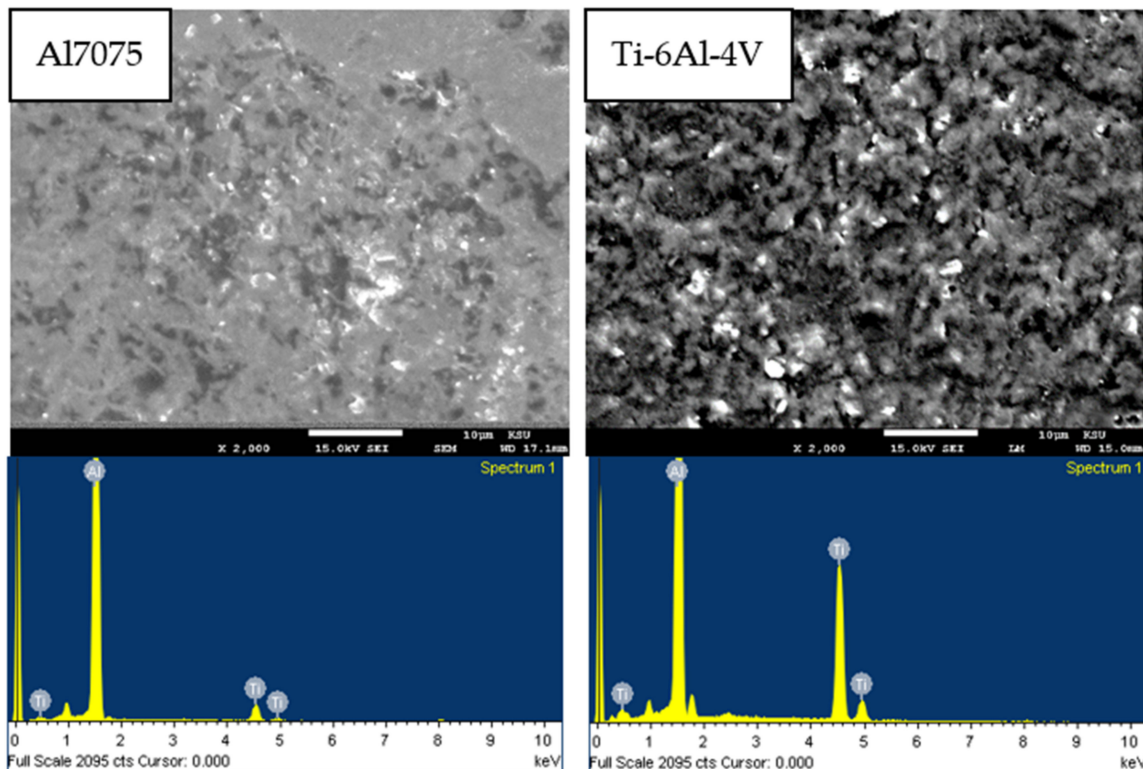

Figure 6. SEM images with the corresponding area scan EDS of the fractured surfaces for bond made at 520 °C holding time.

3.3. Bond Strength Evaluation

The strength of the bonds was evaluated using compressive machine (Instron 5969). The stress corresponding to the maximum load (load at fracture) was evaluated using Bluehill 3.22.1373 software. Table 1 shows the strength at maximum load for bonds at different parameters. At the higher pressure of 10 MPa, it was observed that the strength was increasing when the holding temperature increased. Clearly, the bond was weak at 480 °C and this could be due to the fact that Cu remained at the interface and had not completely dissolved, as seen in Figure 1a. The increase in strength to 19.3 MPa was the maximum in our experiments where a complete dissolution of Cu was confirmed by SEM and XRD. At 520 °C and 10 MPa, the joint region was dominated by IMCs based on aluminum and titanium, as observed in the XRD patterns, and the interface is expected to have less porosities compared with other bonds.

Table 1. The strength of bonds at different conditions.

Bonding Parameters	Strength (MPa)
480 °C/10 MPa	8.1
500 °C/10 MPa	15.5
520 °C/10 MPa	19.3
520 °C/5 MPa	16.2

3.4. Effect of Cu on the Joint Formation

Recently, Aslan Miriyev et al. investigated the direct bonding between the two alloys using SPS [14]. When there is no copper, the IMC formation is mainly determined by the diffusion coefficient of the species in the two sides. The diffusion coefficient of Al into Ti and the diffusion coefficient of Ti into Al at 500 °C are reported to be 1×10^{-11} cm^2/s and 5.6×10^{-21} cm^2/s, respectively [3,15]. As Al has a higher diffusion coefficient than Ti, Al$_3$Ti was shown to be the dominant IMC that formed at the interface. Both Al$_3$Ti and AlTi$_3$ were observed at the interface. However, the Al$_3$Ti IMC was dominant, forming a relatively thick interlayer, whose thickness largely depended on the holding time [14]. In addition, the Al$_3$Ti phase forms at the Ti side due to the same reason of the higher diffusion coefficient of Al compared to Ti in this temperature range.

When Cu was introduced, the IMC formation was no longer determined simply by the diffusion coefficient of Al and Ti due to the introduction of Cu atoms. To compare, it was reported that the diffusion coefficients of Cu into Al and into Ti at 500 °C are 2.6×10^{-9} cm^2/s and 5.5×10^{-17} cm^2/s, respectively [3,16]. Therefore, the diffusion coefficient of Cu into Al is much higher than that of Al into Cu (by ~two orders of magnitude). Hence, the introduction of Cu impeded the diffusion of Al into the Ti side, which allowed the formation of IMCs with a higher Ti content as TiAl$_2$ and AlTi$_3$ were also observed as discussed above in the XRD results. These formed IMCs are responsible for the successful bonding between the two alloys as the formation of different intermetallic compounds is important to enhance the hardness of the joint interface [17].

Based on the above results, the bonding scenario can be described as follows. As the temperature and/or pressure increases, Cu diffuses first into both sides. As the diffusion of Cu into Al is much higher compared to Cu into Ti, diffusion into the Al side will dominate. Therefore, Cu will diffuse into Al, partially hindering the smooth diffusion of Al into Ti when there is no interlayer. On the other side, the diffusion rate of Ti at the given temperature is believed to be higher into Cu in particular [3]. Thus, the formation of the other IMCs with more Ti content, namely Al$_2$Ti and AlTi$_3$, was observed at the joint region. Relatively, the highest bond strength is associated with the bond made under 10 MPa and at 520 °C, since less porosities, less remaining Cu, and more IMCs are expected.

Our work can be compared to the work of Kenevisi and Khoie [17], who used transient liquid phase (TLP) bonding to join the two alloys at 500 °C. Both joining surfaces were immersed in acidic solutions in order to remove the native oxide layers. In our study, the two alloys were used directly without any treatment in acidic solutions. As mentioned above, SPS is expected to provide a self-cleaning property from the local sparks/plasma discharges provided by the high-energy DC pulses. The microstructure in our study and in Kenevisi and Khoie (both at ~500 °C) varies greatly. Kenevisi and Khoie used the transient liquid phase (TLP) bonding method, which allows much faster diffusion from both surfaces [18]. The situation is different with SPS as the diffusion of Ti from the Ti-6Al-4V will be much weaker. Therefore, the diffusion of Al (from Al7075, melting point 477 °C) dominated the process and was responsible for the type of IMCs formed at the interface.

3.5. Effect of IMC Morphology and SPS Processing Parameters on the Bond Strength

It has to be pointed out that the relation between the distribution of IMCs and bond strength is not a straightforward relation. As we pointed out above, the formation of IMCs generally enhances the bond strength. This is due in part to the fact that the formation of IMCs is a result of atomic diffusion, which is the essential bonding process. In addition, and very special to our case here, the formation of IMCs is associated with the fragmentation of the Al$_2$O$_3$ oxide layer that usually forms on the Al7075 surface and would rather act as a barrier to diffusion [19,20], which is an advantage of using the SPS technique, as discussed above. These possible enhancements are, however, conditional on a good distribution of the IMCs at the interface (both laterally and across the interface), and on the "degree of absence" of voids and microcracks in the diffusion layer.

The "lateral" homogeneous distribution of IMCs along the interface can be very crucial in determining the bond strength. For example, Xu et al. reported a weak bond strength when the IMCs formed at the periphery only. They used a pre-ultrasonication step to initiate the formation of IMCs at both the peripheral and central areas of the bond, which significantly improved the bond strength [19]. In our case, the IMC morphology was homogenous along the whole interface, thanks to the excellent heat distribution provided by the SPS technique and the relatively small sample size (DIA 10 mm).

The distribution of IMCs "across" the interface is another point of strength in our samples. Without the Cu interlayer, the diffusion layer at the Ti-6Al-4V/Al7075 interface, as comprehensively studied by Miriyev et al. [14], is a thick continuous layer of Al_3Ti IMC between the two alloys. For a long diffusion time, this kind of single IMC morphology is not preferable as the bond strength can deteriorate with increasing thickness [21]. In our case, the introduction of Cu broke the conditions of this morphology and resulted in a slower diffusion of Al into Ti, allowing the formation of other Ti-rich IMCs.

On the other hand, the above advantages of IMCs are opposed by other drawbacks that may deteriorate the bond strength. For example, the difference between the diffusion coefficient values can result in a net flux of vacancies (the Kirkendall effect) [22]. These vacancies have the tendency to condense with each other and form voids in the joint area. Voids result in a concentration of stress and therefore expansion of the crack, thus weakening the bond. In addition, the difference in thermal expansion between the parent materials and the formed IMCs can result in microcracks along the interface. IMCs form at high temperatures; when the joint cools down, this difference in thermal coefficients can result in a residual stress along the interface, forming internal cracks where a fracture can very probably initiate [23].

In our samples, we did have microcracks and voids. However, the negative effect of voids/microcracks was always efficiently compensated by the obtained IMC distribution. This can be deduced from the systematic enhancement of bond strength with increasing temperature and pressure, which can be explained as follows. At high temperature/pressure conditions, the growth rate of IMC grains in the diffusion layer is expected to increase. This should enhance the development of more voids and microcracks resulting in a weakening of the bond strength, as discussed above. However, the IMC morphology developed in our samples (i.e., a variety of different Ti-Al IMCs with forceful diffusion of Cu into the Al side) had a stronger bond enhancing effect, causing the bond strength to systematically increase with both temperature and pressure, as can be seen in Table 1.

4. Conclusions

In conclusion, spark plasma sintering was successfully used to join Al7075 and Ti-6Al-4V industrial alloys by using a copper foil as an interlayer without the need of a prior process such as surface coatings. Substantial diffusion of copper into the Al7075 region was observed that was highly sensitive to the SPS processing conditions. In particular, both temperature and pressure enhances copper diffusion, and a complete diffusion of copper from the interface down to ~80 μm deep into the aluminum region could be achieved at 520 °C and 10 MPa. This observation suggests that copper does not play a major role in the joining process, a result suggested by the formation of only Al-Ti IMCs at the interface with no Cu-based alloys. The existence of copper could, however, impede the diffusion of Al into Ti at the the early stage, allowing the formation of Ti-Al IMCs with higher Ti content and an enhancement of bond strength.

Future research will involve a study of the effect of holding time on the formation of the IMCs at the joint region. Furthermore, an exploration of using other interlayers to enhance and improve the joining of Al7075 and Ti-6Al-4V alloys and an investigation of the mechanism of diffusion and the microstructural formation of the joint region will be conducted.

References

1. Prescott, R.; Graham, M.J. The formation of aluminum oxide scales on high-temperature alloys. *Oxid. Met.* **1992**, *38*, 233–254. [CrossRef]
2. AlHazaa, A.; Khan, T.I.; Haq, I. Transient liquid phase (TLP) bonding of Al7075 to Ti–6Al–4V alloy. *Mater. Charact.* **2010**, *61*, 312–317. [CrossRef]
3. Alhazaa, A.N.; Khan, T.I. Diffusion bonding of Al7075 to Ti–6Al–4V using Cu coatings and Sn–3.6 Ag–1Cu interlayers. *J. Alloys Compd.* **2010**, *494*, 351–358. [CrossRef]
4. Omori, M. Sintering, consolidation, reaction and crystal growth by the spark plasma system (SPS). *Mater. Sci. Eng. A* **2000**, *287*, 183–188. [CrossRef]
5. Cavaliere, P. *Spark Plasma Sintering of Materials: Advances in Processing and Applications*; Springer: Berlin/Heidelberg, Germany, 2019.
6. Tokita, M. Development of large-size ceramic/metal bulk FGM fabricated by spark plasma sintering. In Proceedings of the Materials Science Forum, Leuven, Belgium, 11–14 July 2004; Volume 308, pp. 83–88.
7. Munir, Z.A.; Anselmi-Tamburini, U.; Ohyanagi, M. The effect of electric field and pressure on the synthesis and consolidation of materials: A review of the spark plasma sintering method. *J. Mater. Sci.* **2006**, *41*, 763–777. [CrossRef]
8. Groza, J.R. Nanosintering. *Nanostruct. Mater.* **1999**, *12*, 987–992. [CrossRef]
9. Manière, C.; Nigito, E.; Durand, L.; Weibel, A.; Beynet, Y.; Estournes, C. Spark plasma sintering and complex shapes: The deformed interfaces approach. *Powder Technol.* **2017**, *320*, 340–345. [CrossRef]
10. Nisar, A.; Zhang, C.; Boesl, B.; Agarwal, A. Unconventional materials processing using spark plasma sintering. *Ceramics* **2021**, *4*, 20–39. [CrossRef]
11. Tokita, M. Progress of Spark Plasma Sintering (SPS) Method, Systems, Ceramics Applications and Industrialization. *Ceramics* **2021**, *4*, 160–198. [CrossRef]
12. Paygin, V.; Dvilis, E.; Alishin, T.; Stepanov, S.; Khasanov, O.; Valiev, D.; Ferrari, M. Application of collector pressing method to manufacture various optically transparent oxide ceramics using SPS technique. *Opt. Mater.* **2022**, *128*, 112332. [CrossRef]
13. Armstrong, J.T. Citzaf-a package of correction programs for the quantitative Electron Microbeam X-Ray-Analysis of thick polished materials, thin-films, and particles. *Microbeam Anal.* **1995**, *4*, 177–200.
14. Miriyev, A.; Levy, A.; Kalabukhov, S.; Frage, N. Interface evolution and shear strength of Al/Ti bi-metals processed by a spark plasma sintering (SPS) apparatus. *J. Alloys Compd.* **2016**, *678*, 329–336. [CrossRef]
15. Askill, J. *Tracer Diffusion Data for Metals, Alloys, and Simple Oxides*; Springer Science & Business Media: Berlin, Germany, 1970; Volume 31, pp. 87–91.
16. Wöhlbier, F. *Diffusion and Defect Data*; Trans Tech Publications: Wollerau, Switzerland, 1971; Volume 5, pp. 121–128.
17. Kenevisi, M.S.; Khoie, M. A study on the effect of bonding time on the properties of Al7075 to Ti–6Al–4V diffusion bonded joint. *Mater. Lett.* **2012**, *76*, 144–146. [CrossRef]
18. AlHazaa, A.; Alhoweml, I.; Shar, M.A.; Hezam, M.; Abdo, H.S.; AlBrithen, H. Transient liquid phase bonding of Ti-6Al-4V and Mg-AZ31 alloys using Zn coatings. *Materials* **2019**, *12*, 769. [CrossRef] [PubMed]
19. Xu, H.; Acoff, V.L.; Liu, C.; Silberschmidt, V.V.; Chen, Z. Facilitating intermetallic formation in wire bonding by applying a pre-ultrasonic energy. *Microelectron. Eng.* **2011**, *88*, 3155–3157. [CrossRef]
20. Xu, H.; Liu, C.; Silberschmidt, V.V.; Pramana, S.S.; White, T.J.; Chen, Z.; Sivakumar, M.; Acoff, V.L. A micromechanism study of thermosonic gold wire bonding on aluminum pad. *J. Appl. Phys.* **2010**, *108*, 113517. [CrossRef]
21. Zhang, D.; Qin, G.; Ma, H.; Geng, P. Non-uniformity of intermetallic compounds and properties in inertia friction welded joints of 2A14 Al alloy to 304 stainless steel. *J. Manuf. Process.* **2021**, *68*, 834–842. [CrossRef]
22. Sequeira, C.A.C.; Amaral, L. Role of Kirkendall effect in diffusion processes in solids. *Trans. Nonferrous Met. Soc. China* **2014**, *24*, 1–11. [CrossRef]
23. Wang, Q.; Leng, X.S.; Yang, T.H.; Yan, J.C. Effects of FeAl intermetallic compounds on interfacial bonding of clad materials. *Trans. Nonferrous Met. Soc. China* **2014**, *24*, 279–284. [CrossRef]